A multi-physical structure-preserving method and its analysis for the conservative Allen-Cahn equation with nonlocal constraint

Xu Liu
Nanjing University of Aeronautics and Astronautics
Qi Hong
Nanjing University of Aeronautics and Astronautics
Hong-lin Liao
Nanjing University of Aeronautics and Astronautics
Yuezheng Gong (gongyuezheng@nuaa.edu.cn)
Nanjing University of Aeronautics and Astronautics

Research Article

Keywords: Conservative Allen-Cahn equation, Energy dissipation law, Maximum bound principle, Multi-physical structure-preserving method, Linear iteration, Error estimate

Posted Date: August 18th, 2023

DOI: https://doi.org/10.21203/rs.3.rs-3253782/v1

Additional Declarations: No competing interests reported.

Version of Record: A version of this preprint was published at Numerical Algorithms on February 3rd, 2024. See the published version at https://doi.org/10.1007/s11075-024-01757-4.

A multi-physical structure-preserving method and its analysis for the conservative Allen-Cahn equation with nonlocal constraint

Xu Liu[1,2], Qi Hong[1,2], Hong-lin Liao[1,2], Yuezheng Gong[1,2*]

[1*]School of Mathematics, Nanjing University of Aeronautics and Astronautics, Nanjing, 211106, China.
[2]Key Laboratory of Mathematical Modelling and High Performance Computing of Air Vehicles (NUAA), MIIT, Nanjing, 211106, China.

*Corresponding author(s). E-mail(s): gongyuezheng@nuaa.edu.cn;
Contributing authors: liuxuljr@163.com; qhong@nuaa.edu.cn;
liaohl@nuaa.edu.cn;

Abstract

The conservative Allen-Cahn equation satisfies three important physical properties, namely the mass conservation law, the energy dissipation law and the maximum bound principle. However, very few numerical methods can preserve them at the same time. In this paper, we present a multi-physical structure-preserving method for the conservative Allen-Cahn equation with nonlocal constraint by combining the averaged vector field method in time and the central finite difference scheme in space, which can conserve all three properties simultaneously at the fully discrete level. We propose an efficient linear iteration algorithm to solve the presented nonlinear scheme, and prove that the iteration satisfies the maximum bound principle and a contraction mapping property in the discrete $\boldsymbol{L}^{\infty}$ norm. Furthermore, concise error estimates in the maximum norm are established on nonuniform time meshes. The theoretical findings of the proposed scheme are verified by several benchmark examples, where an adaptive time-stepping strategy is employed.

Keywords: Conservative Allen-Cahn equation, Energy dissipation law, Maximum bound principle, Multi-physical structure-preserving method, Linear iteration, Error estimate

MSC Classification: 65M06 , 65M12 , 65M70

1 Introduction

For many important phenomena in science and engineering, the corresponding processes are driven by minimizing the free energy through dissipative dynamics [1–5]. Gradient flow models are usually used to investigate these phenomena, where the classical Allen-Cahn (AC) equation and Cahn-Hilliard (CH) equation are two well-known prototypical examples. The classical AC equation is easier to solve numerically than the CH equation due to the low order spatial derivatives, but it does not preserve the mass conservation law, which is still desirable to maintain in many applications [6, 7]. By adding a nonlocal Lagrange multiplier, Rubinstein and Sternberg introduced a conservative AC model [8], which could not only keep the mass conservation, but also satisfy the energy dissipation law and the maximum bound principle [9]. In this paper, we will focus on developing and analyzing a multi-physical structure-preserving scheme for the conservative AC equation.

Consider the binary material occupying a smooth domain $\Omega \subseteq \mathbb{R}^d$, $d = 2$ or 3. The free energy of the system is denoted as

$$E[\phi] = \int_\Omega \left(\frac{\epsilon^2}{2} |\nabla \phi|^2 + F(\phi) \right) \mathrm{d}\boldsymbol{x}, \tag{1.1}$$

where ϕ is the phase variable, ϵ denotes the interface width parameter and $F(\phi)$ is the associated nonlinear potential function. One usually concerns with two typical potential functions, including the standard double-well (Ginzburg-Landau) potential function

$$F(\phi) = \frac{1}{4}(\phi^2 - 1)^2, \tag{1.2}$$

and the logarithmic Flory-Huggins potential function

$$F(\phi) = \frac{\theta}{2}[(1+\phi)\ln(1+\phi) + (1-\phi)\ln(1-\phi)] - \frac{\theta_c}{2}\phi^2, \tag{1.3}$$

where θ and θ_c are two constants satisfying $0 < \theta < \theta_c$. Then the conservative AC equation with a nonlocal constraint is given by [8, 9]

$$\partial_t \phi = \epsilon^2 \Delta \phi + f(\phi) - \frac{1}{|\Omega|} \int_\Omega f(\phi) \mathrm{d}\boldsymbol{x}, \quad \boldsymbol{x} \in \Omega, \quad t > 0, \tag{1.4}$$

with the initial value

$$\phi(\boldsymbol{x}, 0) = \phi_0(\boldsymbol{x}), \quad \boldsymbol{x} \in \overline{\Omega}, \tag{1.5}$$

where $f(\phi) = -F'(\phi)$. Under the periodic or homogeneous Neumann boundary conditions, the model satisfies the mass conservation law

$$\frac{\mathrm{d}}{\mathrm{d}t} \int_\Omega \phi \mathrm{d}\boldsymbol{x} = 0, \tag{1.6}$$

and the energy dissipation law

$$\frac{\mathrm{d}}{\mathrm{d}t}E[\phi] = -\int_{\Omega} |\partial_t \phi|^2 \mathrm{d}\boldsymbol{x} \leq 0. \tag{1.7}$$

More importantly, it has one more maximum bound principle (MBP) property than the CH model [9, 10]. Therefore, the conservative AC model can serve as an excellent alternative to the CH model for simulating interfacial dynamics of immiscible multi-component material systems.

Along the numerical front of structure-preserving algorithms [11], it is always desirable even essential to design energy stable schemes or MBP-preserving methods for the conservative AC equation. For general gradient flow models, there have been many approaches to guide the design of energy stable schemes, including the convex splitting methods [12–14], the stabilizing techniques [15, 16], the fully implicit structure-preserving schemes [17, 18] and the energy quadratization approaches (IEQ, SAV and their variants) [19–23], etc. Recently, Cheng et al. proposed some Lagrange multiplier approaches for constructing structure-preserving schemes [24–26] and Gong et al. developed a supplementary variable method for thermodynamically consistent partial differential equations [27, 28]. However, there are relatively few energy stable schemes for the conservative AC equation. A set of second-order energy stable schemes for the conservative AC equation has been presented and compared with results of the CH model [29, 30]. Some high-order energy stable schemes have been also proposed for the conservative AC model [31, 32].

In addition to energy stable schemes, there have been many studies devoted to MBP-preserving methods for the classical AC equation. To our best knowledge, the numerical strategies used to develop the MBP-preserving schemes in previous works can be classified into four broad categories, including the matrix-vector augment [33], the discrete lower and upper solutions technique [34], the operator splitting strategy [35] and the stabilized exponential time differencing method [36]. The standard trapezoidal Crank-Nicolson scheme for the fractional-in-space AC model was shown to preserve the discrete MBP under some time-step constraints [37]. Liao et al. proved that the variable-step BDF2 method on nonuniform time meshes could preserve the discrete MBP [38]. Recently, we developed a MBP-preserving iteration technique for a class of semilinear parabolic equations [39]. More generally, Du et al. established an abstract framework on the preservation of MBP for a large family of semilinear parabolic equations [10]. However, MBP-preserving numerical methods for the conservative AC equation are still rare. More recently, Li et al. presented two unconditionally MBP-preserving linear schemes for the conservative AC equation based on the stabilized exponential time differencing method [9].

Most of the existing methods can preserve only one physical structure between the energy stability and the MBP property, and few numerical schemes can retain more than two physical structures solving the conservative AC model. In this paper, we develop a multi-physical structure-preserving algorithm for the conservative AC equation by embracing the averaged vector field method in time and the second-order central finite difference scheme in space. Based on the analysis of structure-preserving algorithms, the proposed scheme is proved to conserve the mass conservation law and

the energy dissipation law at the fully discrete level. However, because the proposed scheme is nonlinear, its existence, uniqueness and convergence analysis are faced with great challenges. Inspired by the MBP-preserving iteration technique in Ref. [39], we design a new MBP-preserving linear iteration algorithm for solving the proposed scheme. The iteration is proved to satisfy the MBP and a contraction mapping property under some mild conditions, which imply that the proposed scheme maintains the MBP property and is uniquely solvable. Therefore, our proposed scheme simultaneously preserves the mass conservation law, energy dissipation law and MBP of the conservative AC model. Finally, some numerical experiments are presented to demonstrate the accuracy and multiple physical structures of the proposed algorithm.

The remainder of the paper is organized as follows. Some notations and useful lemmas are introduced and the multi-physical structure-preserving scheme is presented in Section 2. The proposed scheme is proved to preserve the discrete mass conservation law, energy dissipation law and MBP as well as the unique solvability in Section 3. Section 4 presents some concise error estimates in the maximum norm by virtue of the associated MBP property. In Section 5, several numerical examples are carried out to demonstrate the accuracy and multi-physical structures of the proposed scheme. Finally, some conclusions are drawn in Section 6.

2 Multi-physical structure-preserving method

In this section, we will introduce some notations and useful lemmas, and present a fully discrete multi-physical structure-preserving algorithm for the conservative Allen-Cahn model with periodic boundary condition. To simplify the presentation, we focus on the two-dimensional problem. It should be noted that the results of this paper are also applicable to the three-dimensional case.

Let $\Omega = [a, a + L_x] \times [b, b + L_y]$, where for simplicity, we assume $L_x = L_y = L > 0$. Let N be a given positive integer, and define grid spacing $h = L/N$. Then the space domain is uniformly partitioned with the spatial grid points

$$\Omega_h = \big\{(x_j, y_k) | x_j = a + jh,\ y_k = b + kh,\ 0 \le j, k \le N - 1\big\}.$$

Consider the nonuniform time grids $0 = t_0 < t_1 < \cdots < t_n < t_{n+1} < \cdots < t_{N_t} = T$ with the step sizes $\tau_n = t_{n+1} - t_n$ for $0 \le n \le N_t - 1$. Let the maximum time-step size $\tau = \max\limits_{0 \le n < N_t} \tau_n$.

Let $\mathbb{V}_h = \big\{u | u = \{u_{j,k} | (x_j, y_k) \in \Omega_h\}\big\}$ be the space of grid functions on Ω_h. For any two grid functions $u, v \in \mathbb{V}_h$, define the discrete inner product, L^2 norm and maximum norm, respectively,

$$(u, v)_h = h^2 \sum_{j=0}^{N-1} \sum_{k=0}^{N-1} u_{j,k} v_{j,k}, \quad \|u\|_h = \sqrt{(u, u)_h}, \quad \|u\|_\infty = \max_{0 \le j,k \le N-1} |u_{j,k}|.$$

According to Ref. [9], we assume that the nonlinear function f in (1.4) satisfies

$$\exists \beta > 0, \ \ni f(\beta) \le f(w) \le f(-\beta),\ \forall w \in [-\beta, \beta]. \tag{2.1}$$

For the positive constant β, we define the maximum norm space

$$\mathbb{V}_\beta = \Big\{ u \big| \|u\|_\infty \le \beta,\ u \in \mathbb{V}_h \Big\},$$

and the stabilizing constant κ such that

$$\kappa \ge \max_{|w| \le \beta} |f'(w)|. \tag{2.2}$$

For $u \in \mathbb{V}_h$, the discrete Laplace operator is defined by

$$\Delta_h u_{j,k} = \frac{u_{j+1,k} - 2u_{j,k} + u_{j-1,k}}{h^2} + \frac{u_{j,k+1} - 2u_{j,k} + u_{j,k-1}}{h^2}, \quad 0 \le j,k \le N-1,$$

where we note $u_{-1,k} := u_{N-1,k}$, $u_{N,k} := u_{0,k}$, $u_{j,-1} := u_{j,N-1}$, $u_{j,N} := u_{j,0}$ for periodic boundary conditions. For $u \in \mathbb{V}_h$, define the function $f_h(u) \in \mathbb{V}_h$ with the elements

$$\Big(f_h(u)\Big)_{j,k} = f(u_{j,k}), \quad 0 \le j,k \le N-1.$$

Now we apply the second-order center finite difference method in space for the conservative Allen-Cahn equation and obtain the following semi-discrete system

$$\frac{\mathrm{d}\phi}{\mathrm{d}t} = \epsilon^2 \Delta_h \phi + f_h(\phi) - \frac{1}{|\Omega|}\big(f_h(\phi), 1\big)_h, \tag{2.3}$$

where $\phi \in \mathbb{V}_h$. For $u, v \in \mathbb{V}_h$, we define the function $f_d(u,v) \in \mathbb{V}_h$ as

$$f_d(u,v) = \int_0^1 f_h\big((1-\xi)u + \xi v\big)\mathrm{d}\xi.$$

Employing the average vector field method [40] to the system (2.3), we derive the fully discrete multi-physical structure-preserving scheme

$$\frac{\phi^{n+1} - \phi^n}{\tau_n} = \epsilon^2 \Delta_h \frac{\phi^n + \phi^{n+1}}{2} + f_d(\phi^n, \phi^{n+1}) - \frac{1}{|\Omega|}\Big(f_d(\phi^n, \phi^{n+1}), 1\Big)_h. \tag{2.4}$$

We note that the proposed scheme (2.4) can conserve the mass conservation law, the energy dissipation law and the maximum bound principle at the fully discrete level, and is uniquely solvable, which will be analyzed in detail in the next section. To facilitate the analysis of the proposed scheme, we next introduce some useful lemmas.

Lemma 2.1. *For $u, v \in \mathbb{V}_h$, it holds that*

$$(\Delta_h u, v)_h = (u, \Delta_h v)_h. \tag{2.5}$$

Lemma 2.2. *For $u \in \mathbb{V}_h$, it holds that*

(1) $\Delta_h u_{j,k} \le 0$ *if* $u_{j,k} = \max\limits_{(x_l,y_m)\in\Omega_h} u_{l,m}$;

(2) $\Delta_h u_{j,k} \ge 0$ *if* $u_{j,k} = \min\limits_{(x_l,y_m)\in\Omega_h} u_{l,m}$.

Lemma 2.3. *For $u \in \mathbb{V}_h$, it holds that*

$$\frac{2d}{h^2}\Big(- \|u\|_\infty - u_{j,k}\Big) \le \Delta_h u_{j,k} \le \frac{2d}{h^2}\Big(\|u\|_\infty - u_{j,k}\Big), \quad \forall 0 \le j,k \le N-1,$$

where $d = 2$ denotes the spatial dimension. Specially, one has for $u \in \mathbb{V}_\beta$

$$\frac{2d}{h^2}\Big(- \beta - u_{j,k}\Big) \le \Delta_h u_{j,k} \le \frac{2d}{h^2}\Big(\beta - u_{j,k}\Big), \quad \forall 0 \le j,k \le N-1.$$

Lemma 2.4. *For $u, v \in \mathbb{V}_h$, we define the function $N_d(u,v) \in \mathbb{V}_h$ as*

$$N_d(u,v) = \kappa\frac{u+v}{2} + f_d(u,v) - \frac{1}{|\Omega|}\Big(f_d(u,v),1\Big)_h. \tag{2.6}$$

Under the conditions (2.1) and (2.2), the function N_d satisfies

(1) $\|N_d(u,v)\|_\infty \le \kappa\beta, \quad \forall u, v \in \mathbb{V}_\beta,$

(2) $\|N_d(u_1,v_1) - N_d(u_2,v_2)\|_\infty \le \frac{3\kappa}{2}\big(\|u_1-u_2\|_\infty + \|v_1-v_2\|_\infty\big), \quad \forall u_1,u_2,v_1,v_2 \in \mathbb{V}_\beta.$

Proof. For $u \in \mathbb{V}_h$, we define the function $N_h(u) \in \mathbb{V}_h$ as

$$N_h(u) = \kappa u + f_h(u) - \frac{1}{|\Omega|}\Big(f_h(u),1\Big)_h.$$

It is readily to check that

$$N_d(u,v) = \int_0^1 N_h\big((1-\xi)u + \xi v\big)\mathrm{d}\xi.$$

From (2.2), we have

$$\kappa + f'(w) \ge 0, \quad \forall w \in [-\beta,\beta],$$

and thus

$$-\kappa\beta + f(-\beta) \le \kappa w + f(w) \le \kappa\beta + f(\beta), \quad \forall w \in [-\beta,\beta].$$

It follows (2.1) that

$$f(\beta) \le \frac{1}{|\Omega|}\Big(f_h(u),1\Big)_h \le f(-\beta), \quad \forall u \in \mathbb{V}_\beta.$$

According to the two inequalities above, one can obtain

$$-\kappa\beta \le \kappa w + f(w) - \frac{1}{|\Omega|}\Big(f_h(u),1\Big)_h \le \kappa\beta, \quad \forall w \in [-\beta,\beta],\ u \in \mathbb{V}_\beta,$$

which implies

$$\|N_h(u)\|_\infty \le \kappa\beta, \quad \forall u \in \mathbb{V}_\beta.$$

For $u, v \in \mathbb{V}_\beta$ and $\xi \in [0,1]$, we have $(1-\xi)u + \xi v \in \mathbb{V}_\beta$ and deduce

$$\|N_d(u,v)\|_\infty \le \int_0^1 \|N_h\big((1-\xi)u + \xi v\big)\|_\infty \mathrm{d}\xi \le \kappa\beta.$$

Furthermore, we also have from (2.2)

$$|f(w_1) - f(w_2)| \le \kappa |w_1 - w_2|, \quad \forall w_1, w_2 \in [-\beta, \beta],$$

which leads to

$$\|f_h(u_1) - f_h(u_2)\|_\infty \le \kappa \|u_1 - u_2\|_\infty, \quad \forall u_1, u_2 \in \mathbb{V}_\beta.$$

For $u_1, u_2, v_1, v_2 \in \mathbb{V}_\beta$, $\xi \in [0,1]$, denoting $\theta_1(\xi) = (1-\xi)u_1 + \xi v_1$ and $\theta_2(\xi) = (1-\xi)u_2 + \xi v_2$, we have $\theta_1(\xi), \theta_2(\xi) \in \mathbb{V}_\beta$ and thus obtain

$$\begin{aligned}
&\big\|N_h\big(\theta_1(\xi)\big) - N_h\big(\theta_2(\xi)\big)\big\|_\infty \\
\le& \|\kappa\theta_1(\xi) - \kappa\theta_2(\xi)\|_\infty + \big\|f_h\big(\theta_1(\xi)\big) - f_h\big(\theta_2(\xi)\big)\big\|_\infty + \left|\frac{1}{|\Omega|}\left(f_h\big(\theta_1(\xi)\big) - f_h\big(\theta_2(\xi)\big), 1\right)_h\right| \\
\le& 3\kappa \|\theta_1(\xi) - \theta_2(\xi)\|_\infty . \qquad (2.7)
\end{aligned}$$

Note that

$$\|\theta_1(\xi) - \theta_2(\xi)\|_\infty \le (1-\xi)\|u_1 - u_2\|_\infty + \xi\|v_1 - v_2\|_\infty. \qquad (2.8)$$

Combining (2.7) and (2.8) leads to

$$\begin{aligned}
\|N_d(u_1, v_1) - N_d(u_2, v_2)\|_\infty &\le \int_0^1 \big\|N_h\big(\theta_1(\xi)\big) - N_h\big(\theta_2(\xi)\big)\big\|_\infty \,\mathrm{d}\xi \\
&\le \frac{3\kappa}{2}\left(\|u_1 - u_2\|_\infty + \|v_1 - v_2\|_\infty\right),
\end{aligned}$$

which completes the proof. □

3 Multiple-physical structures and unique solvability of the scheme

In this section, the proposed method is first shown to maintain the mass conservation law and the energy dissipation law at the fully discrete level. Then a MBP-preserving linear iteration technique is presented to analyze the MBP-preserving property and unique solvability of the scheme.

Theorem 3.1. *The scheme (2.4) preserves the discrete mass conservation law*

$$(\phi^{n+1}, 1)_h = (\phi^n, 1)_h, \tag{3.1}$$

and the discrete energy dissipation law

$$\frac{E_h[\phi^{n+1}] - E_h[\phi^n]}{\tau_n} = -\left\| \frac{\phi^{n+1} - \phi^n}{\tau_n} \right\|_h^2, \tag{3.2}$$

where the discrete energy is given by

$$E_h[\phi^n] = -\frac{\epsilon^2}{2}(\Delta_h \phi^n, \phi^n)_h + (F_h(\phi^n), 1)_h, \tag{3.3}$$

with the function $F_h(u) \in \mathbb{V}_h$ defined as

$$\Big(F_h(u)\Big)_{j,k} = F(u_{j,k}), \quad 0 \le j, k \le N-1.$$

Proof. According to Lemma 2.1, one has

$$\left(\Delta_h \frac{\phi^n + \phi^{n+1}}{2}, 1\right) = \left(\frac{\phi^n + \phi^{n+1}}{2}, \Delta_h 1\right) = 0.$$

It is easy to check that

$$\left(f_d(\phi^n, \phi^{n+1}) - \frac{1}{|\Omega|}\Big(f_d(\phi^n, \phi^{n+1}), 1\Big)_h, 1\right) = 0.$$

Thus, we take a discrete inner product of (2.4) with 1 and obtain

$$(\phi^{n+1}, 1)_h = (\phi^n, 1)_h.$$

According to the Leibniz formula and Lemma 2.1, one can deduce

$$\begin{aligned} E_h[\phi^{n+1}] - E_h[\phi^n] &= \int_0^1 \frac{\mathrm{d}}{\mathrm{d}\xi} E_h\left[(1-\xi)\phi^n + \xi\phi^{n+1}\right] \mathrm{d}\xi \\ &= \left(-\epsilon^2 \Delta_h \frac{\phi^n + \phi^{n+1}}{2} - f_d(\phi^n, \phi^{n+1}), \phi^{n+1} - \phi^n\right)_h \\ &= \left(-\epsilon^2 \Delta_h \frac{\phi^n + \phi^{n+1}}{2} - f_d(\phi^n, \phi^{n+1}) + \frac{1}{|\Omega|}(f_d(\phi^n, \phi^{n+1}), 1), \phi^{n+1} - \phi^n\right)_h, \end{aligned} \tag{3.4}$$

where the last step is attributed to the discrete mass conservation law. Substituting (2.4) into (3.4) leads to

$$E_h[\phi^{n+1}] - E_h[\phi^n] = -\tau_n \left\| \frac{\phi^{n+1} - \phi^n}{\tau_n} \right\|_h^2, \tag{3.5}$$

which gives the discrete energy dissipation law and completes the proof. □

Although the nonlinear scheme (2.4) has been proved to be mass-preserving and energy-dissipation-preserving, two problems should be answered, one is whether its solution is unique, and the other is how to develop a convergent linear iterative algorithm to compute it. In addition, it is also challenge to analyze the discrete MBP-preserving property of the scheme. To these ends, we design a MBP-preserving linear iteration technique for the nonlinear scheme (2.4). Firstly, we reformulate the proposed method (2.4) into the following equivalent form

$$\frac{\phi^{n+1} - \phi^n}{\tau_n} = \epsilon^2 \Delta_h \frac{\phi^n + \phi^{n+1}}{2} - \kappa \frac{\phi^n + \phi^{n+1}}{2} + N_d(\phi^n, \phi^{n+1}), \tag{3.6}$$

where the definition of N_d is given by (2.6). Subsequently, we present the following linear iteration method for solving (3.6)

$$\frac{\phi_{(s+1)}^{n+1} - \phi^n}{\tau_n} = \epsilon^2 \Delta_h \frac{\phi^n + \phi_{(s+1)}^{n+1}}{2} - \kappa \frac{\phi^n + \phi_{(s+1)}^{n+1}}{2} + N_d(\phi^n, \phi_{(s)}^{n+1}), \quad s \geq 0, \tag{3.7}$$

where the subscript (s) denotes the sth-iteration step, and the initial iteration is taken as $\phi_{(0)}^{n+1} = \phi^n$.

Theorem 3.2. *Assume that $\phi_{(0)}^{n+1} = \phi^n \in \mathbb{V}_\beta$ and the time-step size τ_n satisfies the following condition*

$$\tau_n \leq \frac{1}{d(\epsilon/h)^2 + \kappa/2}, \tag{3.8}$$

then the solution of the iteration scheme (3.7) satisfies

$$\phi_{(s)}^{n+1} \in \mathbb{V}_\beta, \quad \forall s \geq 0.$$

Proof. By applying the mathematical induction, we assume that $\phi_{(s)}^{n+1} \in \mathbb{V}_\beta$ for fixed s and then prove $\phi_{(s+1)}^{n+1} \in \mathbb{V}_\beta$. On the one hand, suppose that the iteration solution $\phi_{(s+1)}^{n+1}$ reaches its maximum at $(x_j, y_k) \in \Omega_h$, i.e.,

$$\left[\phi_{(s+1)}^{n+1}\right]_{j,k} = \max_{0 \leq l,m \leq N-1} \left[\phi_{(s+1)}^{n+1}\right]_{l,m}. \tag{3.9}$$

According to Lemmas 2.2 and 2.3, it holds for $\phi^n \in \mathbb{V}_\beta$ that

$$\left[\frac{\Delta_h\phi^n + \Delta_h\phi^{n+1}_{(s+1)}}{2}\right]_{j,k} \leq \frac{d}{h^2}\left(\beta - \phi^n_{j,k}\right). \tag{3.10}$$

For $\phi^n, \phi^{n+1}_{(s)} \in \mathbb{V}_\beta$, it follows from Lemma 2.4 that

$$\left\|N_d(\phi^n, \phi^{n+1}_{(s)})\right\|_\infty \leq \kappa\beta. \tag{3.11}$$

Taking the spatial grid point (x_j, y_k) in the iteration scheme (3.7) and combining (3.10) and (3.11), one can derive that

$$\left[\frac{\phi^{n+1}_{(s+1)} - \phi^n}{\tau_n}\right]_{j,k} \leq \left[\frac{d\epsilon^2}{h^2}(\beta - \phi^n) - \kappa\frac{\phi^n + \phi^{n+1}_{(s+1)}}{2}\right]_{j,k} + \kappa\beta, \tag{3.12}$$

which implies

$$\left(\frac{1}{\tau_n} + \frac{\kappa}{2}\right)\left[\phi^{n+1}_{(s+1)}\right]_{j,k} \leq \left(\frac{1}{\tau_n} - \frac{d\epsilon^2}{h^2} - \frac{\kappa}{2}\right)\phi^n_{j,k} + \left(\frac{d\epsilon^2}{h^2} + \kappa\right)\beta. \tag{3.13}$$

Noting that the time-step condition (3.8) is equivalent to

$$\frac{1}{\tau_n} - \frac{d\epsilon^2}{h^2} - \frac{\kappa}{2} \geq 0,$$

thus we have

$$\left(\frac{1}{\tau_n} + \frac{\kappa}{2}\right)\left[\phi^{n+1}_{(s+1)}\right]_{j,k} \leq \left(\frac{1}{\tau_n} - \frac{d\epsilon^2}{h^2} - \frac{\kappa}{2}\right)\beta + \left(\frac{d\epsilon^2}{h^2} + \kappa\right)\beta = \left(\frac{1}{\tau_n} + \frac{\kappa}{2}\right)\beta,$$

which leads to

$$\left[\phi^{n+1}_{(s+1)}\right]_{j,k} \leq \beta. \tag{3.14}$$

On the other hand, suppose that the iteration solution $\phi^{n+1}_{(s+1)}$ achieves its minimum value at (x_p, y_q), i.e., $\left[\phi^{n+1}_{(s+1)}\right]_{p,q} = \min\limits_{0\leq l,m\leq N-1}\left[\phi^{n+1}_{(s+1)}\right]_{l,m}$. By the similar arguments, it is easy to deduce that $\left[\phi^{n+1}_{(s+1)}\right]_{p,q} \geq -\beta$. As a consequence, one has $\phi^{n+1}_{(s+1)} \in \mathbb{V}_\beta$. This completes the proof. □

Theorem 3.3. *Assume that the time-step size τ_n is properly small such that*

$$\tau_n \leq \frac{1}{d(\epsilon/h)^2 + \kappa/2}, \quad \tau_n < \frac{1}{\kappa}, \tag{3.15}$$

then the iteration (3.7) *is convergent.*

Proof. For any grid function $v \in \mathbb{V}_\beta$, it follows from Theorem 3.2 that the iteration (3.7) defines a mapping $T_n : \mathbb{V}_\beta \to \mathbb{V}_\beta$, denoted by $T_n[v] = u \in \mathbb{V}_\beta$, that is,

$$\frac{u-\phi^n}{\tau_n} = \epsilon^2 \Delta_h \frac{\phi^n + u}{2} - \kappa \frac{\phi^n + u}{2} + N_d(\phi^n, v). \tag{3.16}$$

We note that the iteration (3.7) can be rewritten as $\phi^{n+1}_{(s+1)} = T_n[\phi^{n+1}_{(s)}]$. Next, we will prove that T_n is a contraction mapping under the time step restriction (3.15). For any grid functions $v_1, v_2 \in \mathbb{V}_\beta$, we set $u_1 = T_n[v_1], u_2 = T_n[v_2] \in \mathbb{V}_\beta$. Then, one can derive that

$$\frac{\delta u}{\tau_n} = \epsilon^2 \Delta_h \frac{\delta u}{2} - \kappa \frac{\delta u}{2} + N_d(\phi^n, v_1) - N_d(\phi^n, v_2), \tag{3.17}$$

where $\delta u = u_1 - u_2$. Assume that the maximum value of δu is attained at $(x_j, y_k) \in \Omega_h$ such that $\delta u_{j,k} = \max\limits_{l,m} \delta u_{l,m}$. By using Lemmas 2.2 and 2.4, it arrives at

$$\Delta_h \delta u_{j,k} \le 0, \quad \left\| N_d(\phi^n, v_1) - N_d(\phi^n, v_2) \right\|_\infty \le \frac{3\kappa}{2} \|v_1 - v_2\|_\infty. \tag{3.18}$$

Computing (3.17) at (x_j, y_k) and inserting the estimates (3.18), we obtain

$$\left(\frac{1}{\tau_n} + \frac{\kappa}{2} \right) \delta u_{j,k} \le \frac{3\kappa}{2} \|v_1 - v_2\|_\infty.$$

Similarly, one can get

$$\left(\frac{1}{\tau_n} + \frac{\kappa}{2} \right) \delta u_{p,q} \ge -\frac{3\kappa}{2} \|v_1 - v_2\|_\infty,$$

where $\delta u_{p,q} = \min\limits_{l,m} \delta u_{l,m}$. Therefore, the grid function δu can be bounded by

$$\|T_n[v_1] - T_n[v_2]\|_\infty = \|\delta u\|_\infty \le l_n \|v_1 - v_2\|_\infty,$$

where the contraction factor l_n is defined by

$$l_n = \frac{3\kappa\tau_n}{2 + \kappa\tau_n}. \tag{3.19}$$

The time step restriction $\tau_n < 1/\kappa$ implies $l_n < 1$. Thus T_n is a contractive mapping, which implies that the iteration $\phi^{n+1}_{(s+1)} = T_n[\phi^{n+1}_{(s)}]$ is convergent. □

Corollary 3.1. *Under the condition* (3.15)*, the scheme* (2.4) *has a unique solution* $\phi^{n+1} \in \mathbb{V}_\beta$.

Remark 3.1. *The iteration step (3.7) is a system of linear equations with constant coefficients, which can be efficiently computed by the FFT algorithm. The convergence analysis of the iteration guarantees the validity of the scheme (2.4) in practice theoretically.*

Remark 3.2. *To our best knowledge, it is the first time to develop a second-order multi-physical structure-preserving scheme for the conservative AC model, where the mass conservation law, the energy dissipation law and the MBP are conserved simultaneously at the fully discrete level. Thanks to the MBP-preserving linear iteration technique, the proposed fully implicit scheme can be proved to be MBP-preserving and uniquely solvable. Furthermore, although we have presented theoretical results in two-dimensional space, it is straightforward to extend the theory developed in this paper to three-dimensional space.*

4 Maximum norm error estimate

In this section, we will establish the error estimate of the scheme (2.4) in the maximum norm. To this end, we first introduce the following discrete Gronwall inequality [39].

Lemma 4.1. *Consider two positive constants λ_0, λ_1 and let $\lambda = \lambda_0 + \lambda_1$. Assume that the two nonnegative time sequences $\{v^k\}_{k=0}^{N_t}$ and $\{\xi^k\}_{k=0}^{N_t}$ satisfy*

$$v^{n+1} - v^n \le \tau_n(\lambda_0 v^{n+1} + \lambda_1 v^n) + \xi^n \quad \text{for} \quad 0 \le n \le N_t - 1.$$

If the maximum step size $\tau \le 1/(2\lambda_0)$, then

$$v^{n+1} \le \exp(2\lambda t_{n+1}) \left(v^0 + 2 \sum_{j=0}^{n} \xi^j \right) \quad \text{for} \quad 0 \le n \le N_t - 1.$$

Theorem 4.1. *Assume that $\|\phi_0(\mathbf{x})\|_\infty \le \beta$ and the solution $\phi(\mathbf{x}, t)$ of (1.4) is sufficiently smooth such that $\phi \in C^3\left([0,T], C^4(\Omega)\right)$. Suppose further that the condition (3.15) holds such that the scheme (2.4) is uniquely solvable and preserves the discrete MBP. If the maximum time step size $\tau \le \frac{1}{2\kappa}$, the solution ϕ^{n+1} of the scheme (2.4) is convergent in the maximum norm*

$$\|\phi(\cdot, t_{n+1}) - \phi^{n+1}\|_\infty \le 2t_{n+1} \exp(4\kappa t_{n+1}) C_\phi (\tau^2 + h^2) \quad \text{for} \quad 0 \le n \le N_t - 1,$$

where C_ϕ is a constant.

Proof. Let $\Phi^n \in \mathbb{V}_h$ be the exact solution of (1.4) on Ω_h. According to the local truncation error analysis, it is not difficult to check that

$$\frac{\Phi^{n+1} - \Phi^n}{\tau_n} = \epsilon^2 \Delta_h \frac{\Phi^n + \Phi^{n+1}}{2} - \kappa \frac{\Phi^n + \Phi^{n+1}}{2} + N_d(\Phi^n, \Phi^{n+1}) + R^n, \tag{4.1}$$

where the local truncation error satisfies

$$\|R^n\|_\infty \le C_\phi(\tau^2 + h^2). \tag{4.2}$$

Denote the error grid function $e^n = \Phi^n - \phi^n \in \mathbb{V}_h$ for $0 \le n \le N_t$. It is easy to get the following error equation

$$\frac{e^{n+1}-e^n}{\tau_n} = \epsilon^2 \Delta_h \frac{e^n + e^{n+1}}{2} - \kappa \frac{e^n + e^{n+1}}{2} + N_d(\Phi^n, \Phi^{n+1}) - N_d(\phi^n, \phi^{n+1}) + R^n, \quad (4.3)$$

where $e^0 = 0$.

At first, we assume that the maximum value of error function e^{n+1} is achieved at $(x_j, y_k) \in \Omega_h$, i.e.,

$$e^{n+1}_{j,k} = \max_{0 \le l,m \le N-1} e^{n+1}_{l,m}. \quad (4.4)$$

According to Lemma 2.2 and 2.3, it holds that

$$\left[\frac{\Delta_h e^n + \Delta_h e^{n+1}}{2}\right]_{j,k} \le \frac{d}{h^2}\left(\|e^n\|_\infty - e^n_{j,k}\right). \quad (4.5)$$

For $\phi^n, \phi^{n+1}, \Phi^n, \Phi^{n+1} \in \mathbb{V}_\beta$, it follows from Lemma 2.4 that

$$\left\|N_d(\Phi^n, \Phi^{n+1}) - N_d(\phi^n, \phi^{n+1})\right\|_\infty \le \frac{3\kappa}{2}(\|e^n\|_\infty + \|e^{n+1}\|_\infty). \quad (4.6)$$

Taking the spatial grid point (x_j, y_k) in the error equation (4.3) and combining (4.5) and (4.6), we obtain

$$\frac{e^{n+1}_{j,k} - e^n_{j,k}}{\tau_n} \le \frac{d\epsilon^2}{h^2}\left(\|e^n\|_\infty - e^n_{j,k}\right) - \kappa \frac{e^n_{j,k} + e^{n+1}_{j,k}}{2} + \frac{3\kappa}{2}(\|e^n\|_\infty + \|e^{n+1}\|_\infty) + \|R^n\|_\infty, \quad (4.7)$$

which leads to

$$\left(\frac{1}{\tau_n} + \frac{\kappa}{2}\right) e^{n+1}_{j,k} \le \left(\frac{1}{\tau_n} - \frac{d\epsilon^2}{h^2} - \frac{\kappa}{2}\right) e^n_{j,k} + \left(\frac{d\epsilon^2}{h^2} + \frac{3\kappa}{2}\right)\|e^n\|_\infty + \frac{3\kappa}{2}\|e^{n+1}\|_\infty + \|R^n\|_\infty. \quad (4.8)$$

Noticing that $\frac{1}{\tau_n} - \frac{d\epsilon^2}{h^2} - \frac{\kappa}{2} \ge 0$, one can deduce from (4.8) that

$$\left(\frac{1}{\tau_n} + \frac{\kappa}{2}\right) e^{n+1}_{j,k} \le \left(\frac{1}{\tau_n} + \kappa\right)\|e^n\|_\infty + \frac{3\kappa}{2}\|e^{n+1}\|_\infty + \|R^n\|_\infty. \quad (4.9)$$

Similarly, one can derive that

$$\left(\frac{1}{\tau_n} + \frac{\kappa}{2}\right) e^{n+1}_{p,q} \ge -\left(\frac{1}{\tau_n} + \kappa\right)\|e^n\|_\infty - \frac{3\kappa}{2}\|e^{n+1}\|_\infty - \|R^n\|_\infty, \quad (4.10)$$

where $e_{p,q}^{n+1} = \min_{0\le l,m\le N-1} e_{l,m}^{n+1}$. According to $e_{p,q}^{n+1} \le e_{l,m}^{n+1} \le e_{j,k}^{n+1}, \forall l,m$ and (4.9)-(4.10), we obtain

$$\left(\frac{1}{\tau_n}+\frac{\kappa}{2}\right)\|e^{n+1}\|_\infty \le \left(\frac{1}{\tau_n}+\kappa\right)\|e^n\|_\infty + \frac{3\kappa}{2}\|e^{n+1}\|_\infty + \|R^n\|_\infty,$$

which means

$$\|e^{n+1}\|_\infty - \|e^n\|_\infty \le \kappa\tau_n\left(\|e^n\|_\infty + \|e^{n+1}\|_\infty\right) + \tau_n\|R^n\|_\infty.$$

Therefore, for $\tau \le \frac{1}{2\kappa}$, it follows from Lemma 4.1 that

$$\|e^{n+1}\|_\infty \le 2t_{n+1}\exp(4\kappa t_{n+1})C_\phi(\tau^2+h^2), \tag{4.11}$$

which completes the proof. □

5 Numerical experiments

In this section, we focus on the conservative AC equation with the double-well potential function and conduct some numerical examples to substantiate our theoretical analyses on convergence and the properties of multi-physical structures. For the double-well case, it follows Ref. [9] that $\beta = \frac{2\sqrt{3}}{3}$, $\kappa = 3$ and $\epsilon = 0.01$ are chosen in the whole numerical simulations. The MBP-preserving iteration (3.7) is adopted for solving the proposed method (2.4), where the iterative tolerance is set as $Tol = 10^{-14}$. Since the solutions of the conservative AC model exhibit a rich diversity of time scales, the following adaptive time-stepping strategy [41, 42] is considered as follows

$$\tau_{n+1} = \max\left\{\tau_{\min}, \frac{\tau_{\max}}{\sqrt{1+\eta\|\partial_\tau\phi^n\|_h^2}}\right\}, \tag{5.1}$$

where $\partial_\tau\phi^n = (\phi^{n+1}-\phi^n)/\tau_n$, and $\tau_{\max}$, $\tau_{\min}$ denote the predetermined maximum and minimum time steps, as well as η is chosen by the user to adjust the level of adaptivity. Here we choose $\tau_{\max} = 10^{-1}$, $\tau_{\min} = 10^{-3}$ and $\eta = 10^3$.

Example 5.1 (Convergence test)**.** *We solve the conservative AC equation (1.4) with the double-well potential function (1.2) and the following initial condition*

$$\phi_0(x,y) = \cos(2\pi x)\cos(2\pi y), \quad (x,y)\in\Omega, \tag{5.2}$$

where the spatial domain is set as $\Omega = [0,1]\times[0,1]$.

To examine the time accuracy, the reference solution is obtained by using the proposed scheme with a small uniform time-step size $\tau = 10^{-5}$ *and a spatial mesh size* $h = 1/256$. *For fixed* $N = 256$*, we consider a non-uniform time steps* $\tau_{k-1} = T\mu_k/\sum_{k=1}^{N_t}\mu_k$ *for* $1\le k\le N_t$*, where* $\mu_k \in (0,1)$ *are random numbers. The problem is then solved up*

to $T = 1$. The discrete L^∞ error $e(N_t) = \|\phi(\mathbf{x}, T) - \phi^{N_t}\|_\infty$ is recorded in each run and the convergence order is evaluated as follows

$$\text{Order} = \frac{\log\big(e(N_t)/e(2N_t)\big)}{\log\big(\tau(N_t)/\tau(2N_t)\big)}, \tag{5.3}$$

where $\tau(N_t)$ represents the maximum time-step size for N_t. The discrete L^∞ errors are summarized in Table 5.1, where the maximum step ratios $r_{\max} = \max_k \tau_k/\tau_{k-1}$ are also recorded. It can be easily observed that the proposed scheme can reach a second-order accuracy in time.

For the spatial accuracy test, the reference solution is computed by the proposed scheme with $\tau = 10^{-5}$ and $N = 1024$. For fixed $\tau = 10^{-5}$, we choose the $N \times N$ spatial meshes, where $N = 64, 128, 256$ or 512. The problem is then solved up to $T = 0.1$. The corresponding errors in discrete L^∞ norm are summarized in Table 5.2, which clearly indicates that the proposed scheme is of second-order in space. In a word, the numerical performances are quantitatively consistent with our theoretical results.

Table 5.1 Time refinement test on non-uniform meshes ($\epsilon = 0.01$, $\kappa = 3$, $T = 1$, $N = 256$).

N_t	$\tau_{\max}$	$r_{\max}$	$e(N_t)$	Order
20	1.21e-01	34.81	1.08e-04	-
40	4.79e-02	19.47	1.82e-05	1.93
80	2.39e-02	57.12	4.32e-06	2.06
160	1.25e-02	268.66	1.20e-06	1.96

Table 5.2 Space refinement test ($\epsilon = 0.01$, $\kappa = 3$, $T = 0.1$, $\tau = 10^{-5}$).

N	L^∞ error	Order
64	6.3108e-07	-
128	1.5623e-07	2.0141
256	3.7281e-08	2.0642
512	7.4585e-09	2.3215

Example 5.2 (The 2D dynamics)**.** *To test multi-physical structure-preserving properties of the proposed scheme, we simulate merging of four drops with an initial condition given by*

$$\phi_0(x, y) = -\tanh\left(\frac{(x-0.3)^2 + y^2 - 0.2^2}{\epsilon^2}\right)\tanh\left(\frac{(x+0.3)^2 + y^2 - 0.2^2}{\epsilon^2}\right)$$

$$\times \tanh\left(\frac{x^2+(y-0.3)^2-0.2^2}{\epsilon^2}\right)\tanh\left(\frac{x^2+(y+0.3)^2-0.2^2}{\epsilon^2}\right).$$

The computational domain $\Omega=[-1,1]\times[-1,1]$ *is divided uniformly into* 256 *parts in each direction.*

To examine the performance of the proposed scheme in a long time computing, the problem is solved till final time $t=1000$ *by employing the adaptive time-stepping strategy. The profiles of the phase variable at various times are reported in Figure 5.1, where the four drops coalesce into one single drop due to the surface tension effect. Meanwhile, the corresponding evolutions of the mass error, the energy and the supremum norm of the numerical solutions are displayed in Figure 5.2. We observe that the mass is conserved exactly, the energy decays monotonically, and the discrete MBP is warranted. These findings are well consistent with the characteristics of multi-physical structures. As shown in Figure 5.2 (d), the adaptive time step will remain at its maximum value after the steady state is reached, which means that the adaptive strategy is very efficient.*

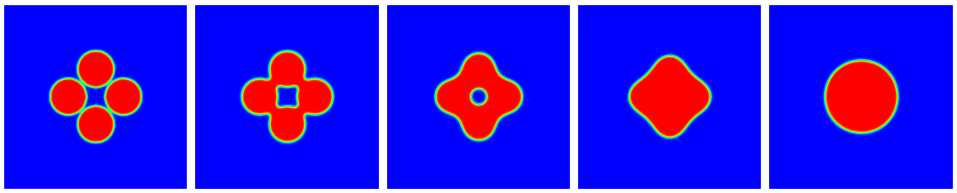

Fig. 5.1 The dynamics of four drops merging at $t=1,10,50,100$ and 1000 ($\epsilon=0.01$, $\kappa=3$, $N=256$).

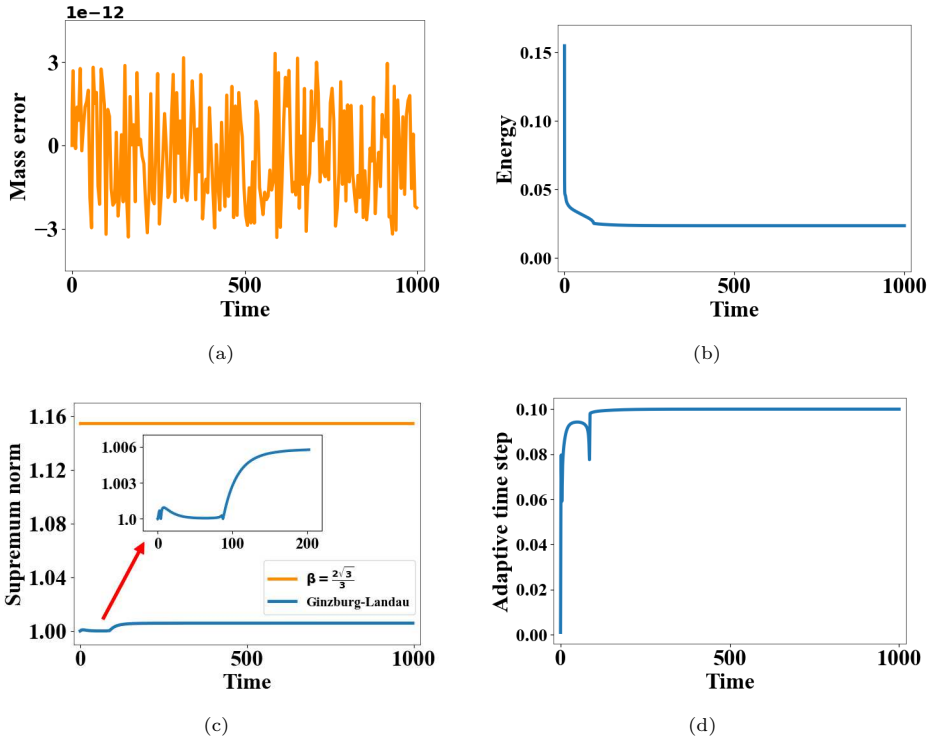

(a) (b) (c) (d)

Fig. 5.2 Evolutions for the 2D dynamics ($\epsilon = 0.01$, $\kappa = 3$, $N = 256$). (a) The mass error; (b) the energy; (c) the supremum norm; (d) the adaptive time step.

Example 5.3 (The 3D dynamics)**.** *In this example, we numerically simulate the evolution of an expanding bubble in three dimensions, governed by the conservative AC equation with the double-well potential function. The initial value is given by*

$$\phi_0(x, y, z) = \begin{cases} -0.5, & x^2 + y^2 + z^2 < 0.25^2, \\ 0.5, & \textit{otherwise}. \end{cases} \tag{5.4}$$

The computational domain $\Omega = [-0.5, 0.5]^3$ *is uniformly partitioned with the spatial mesh size* $h = 1/64$.

We test the scheme (2.4) *in three dimensions with the adaptive time-step strategy. The numerical solutions at* $t = 1, 10, 100, 200$ *are plotted in Figure 5.3, which shows that the bubble increases until a steady state. The evolutions of the mass error, the energy, the supremum norm of the numerical solution and the adaptive time steps are also given in Figure 5.4. It is easy to find that the mass is conserved exactly, the energy decays monotonically, and the MBP is well preserved numerically along the time. Overall, these observations are consistent with the theoretical results.*

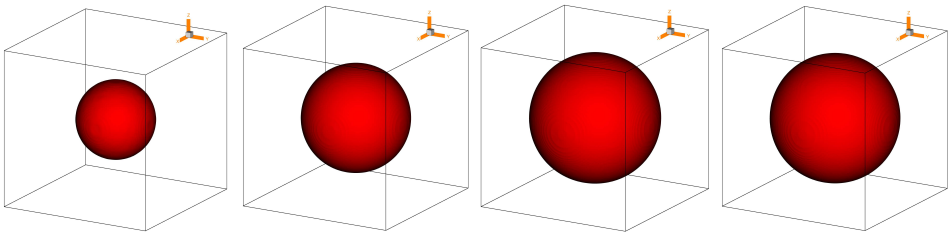

Fig. 5.3 Simulated expanding bubbles at $t = 1, 10, 100, 200$ ($\epsilon = 0.01$, $\kappa = 3$, $N = 64$).

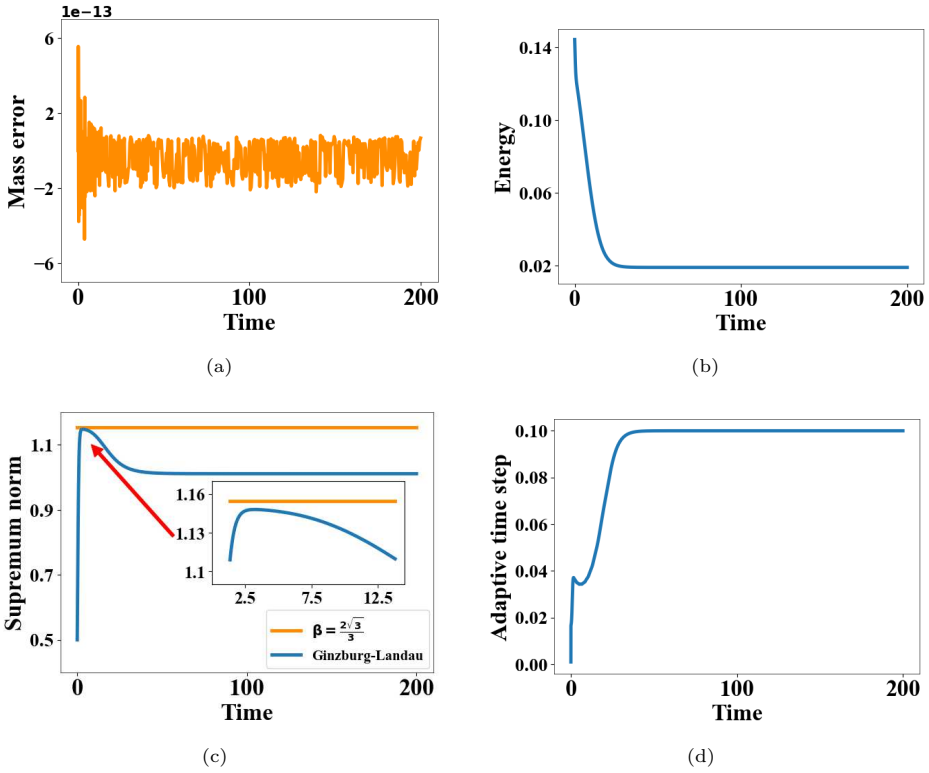

Fig. 5.4 Evolutions for the 3D dynamics ($\epsilon = 0.01$, $\kappa = 3$, $N = 64$). (a) The mass error; (b) the energy; (c) the supremum norm; (d) the adaptive time step.

6 Conclusions

In this paper, we have developed a multi-physical structure-preserving method for solving the conservative AC equation, where the averaged field method in time and the central finite difference scheme in space is implemented. According to the theory of structure-preserving algorithms, we first show that it maintains the mass conservation law and the energy dissipation law at the fully discrete level, consistent with

the continuum theory. A MBP-preserving linear iteration algorithm is then presented for solving the developed method. Surprisingly, this iteration is proved to conserve the discrete MBP and be convergent, which ensures the MBP-preserving property and unique solvability of the developed method. As a result, our scheme simultaneously maintains the mass conservation law, the energy dissipation law and the MBP of the model. Due to the MBP-preserving property, its maximum norm error estimate is further established on non-uniform time meshes. Numerical examples for the conservative AC equation with the double-well potential function are presented to demonstrate that the proposed scheme has second-order accuracy in space-time and conserves the multi-physical properties, and is very efficient especially when coupled with an adaptive time-stepping procedure.

Declarations

- Ethics approval. Not Applicable.
- Availability of supporting data. All data generated or analysed during this study are included in this published article.
- Competing interests. The authors have no conflict of interest.
- Funding. This work is supported by the National Natural Science Foundation of China (Grant Nos. 12271252, 12071216 and 12201297), the Natural Science Foundation of Jiangsu Province (Grant No. BK20220131), the Foundation of Jiangsu Key Laboratory for Numerical Simulation of Large Scale Complex Systems (Grant No. 202002), the Fundamental Research Funds for the Central Universities (Grant No. NS2022070), the LCP Fund for Young Scholar (Grant No. 6142A05QN22005) and Postgraduate Research & Practice Innovation Program of NUAA (Grant No. xcxjh20220804).
- Authors' contributions. All authors contributed equally.
- Acknowledgments. The authors would like to thank the editors and anonymous reviewers.

References

[1] Cahn, J.W., Hilliard, J.E.: Free energy of a nonuniform system. I. interfacial free energy. Journal of Chemical Physics **28**, 258–267 (1958)

[2] Allen, S.M., Cahn, J.W.: A microscopic theory for antiphase boundary motion and its application to antiphase domain coarsening. Acta Metallurgica **27**, 1085–1095 (1979)

[3] Clarke, S., Vvedensky, D.D.: Origin of reflection high-energy electron-diffraction intensity oscillations during molecular-beam epitaxy: A computational modeling approach. Physical Review Letters **58**, 2235–2238 (1987)

[4] Badalassi, V.E., Ceniceros, H.D., Banerjee, S.: Computation of multiphase systems with phase field models. Journal of Computational Physics **190**, 371–397 (2003)

[5] Guo, Z., Yu, F., Lin, P., Wise, S.M., Lowengrub, J.: A diffuse domain method for two-phase flows with large density ratio in complex geometries. Journal of Fluid Mechanics **907**, 38 (2021)

[6] Brassel, M., Bretin, E.: A modified phase field approximation for mean curvature flow with conservation of the volume. Mathematical Methods in the Applied Sciences **34**, 1157–1180 (2011)

[7] Kim, J., Lee, S., Choi, Y.: A conservative Allen-Cahn equation with a space-time dependent Lagrange multiplier. International Journal of Engineering Science **84**, 11–17 (2014)

[8] Rubinstein, J., Sternberg, P.: Nonlocal reaction-diffusion equations and nucleation. IMA Journal of Applied Mathematics **48**, 249–264 (1992)

[9] Li, J., Ju, L., Cai, Y., Feng, X.: Unconditionally maximum bound principle preserving linear schemes for the conservative Allen-Cahn equation with nonlocal constraint. Journal of Scientific Computing **87**, 1–32 (2021)

[10] Du, Q., Ju, L., Li, X., Qiao, Z.: Maximum bound principles for a class of semilinear parabolic equations and exponential time-differencing schemes. SIAM Review **63**, 317–359 (2021)

[11] Hairer, E., Lubich, C., Wanner, G.: Geometric Numerical Integration: Structure-Preserving Algorithms for Ordinary Differential Equations. Springer, ??? (2006)

[12] Eyre, D.J.: Unconditionally gradient stable time marching the Cahn-Hilliard equation. Mrs Online Proceedings Library (OPL) **529**, 39–46 (1998)

[13] Wang, C., Wise, S.M.: An energy stable and convergent finite-difference scheme for the modified phase field crystal equation. SIAM Journal on Numerical Analysis **49**, 945–969 (2011)

[14] Shen, J., Wang, C., Wang, X., Wise, S.M.: Second-order convex splitting schemes for gradient flows with Ehrlich-Schwoebel type energy: Application to thin film epitaxy. SIAM Journal on Numerical Analysis **50**, 105–125 (2012)

[15] Liu, C., Shen, J., Yang, X.: Dynamics of defect motion in nematic liquid crystal flow: modeling and numerical simulation . Communications in Computational Physics **2**, 1184–1198 (2007)

[16] Xu, C., Tang, T.: Stability analysis of large time-stepping methods for epitaxial growth models. SIAM Journal on Numerical Analysis **44**, 1759–1779 (2006)

[17] Du, Q., Nicolaides, R.A.: Numerical analysis of a continuum model of phase transition. SIAM Journal on Numerical Analysis **28**, 1310–1322 (1991)

[18] Furihata, D.: A stable and conservative finite difference scheme for the Cahn-Hilliard equation. Numerische Mathematik **87**, 675–699 (2001)

[19] Yang, X., Zhao, J., Wang, Q.: Numerical approximations for the molecular beam epitaxial growth model based on the invariant energy quadratization method. Journal of Computational Physics **333**, 104–127 (2017)

[20] Shen, J., Xu, J., Yang, J.: The scalar auxiliary variable (SAV) approach for gradient flows. Journal of Computational Physics **353**, 407–416 (2018)

[21] Lin, L., Liu, X., Dong, S.: A gPAV-based unconditionally energy-stable scheme for incompressible flows with outflow/open boundaries. Computer Methods in Applied Mechanics and Engineering **365**, 112969 (2020)

[22] Shen, J., Xu, J., Yang, J.: A new class of efficient and robust energy stable schemes for gradient flows. SIAM Review **61**, 474–506 (2019)

[23] Zhao, J., Yang, X., Gong, Y., Zhao, X., Yang, X., Li, J., Wang, Q.: A general strategy for numerical approximations of non-equilibrium models-Part I: thermodynamical systems. International Journal of Numerical Analysis and Modeling **15**, 884–918 (2018)

[24] Cheng, Q., Liu, C., Shen, J.: A new Lagrange multiplier approach for gradient flows. Computer Methods in Applied Mechanics and Engineering **367**, 113070 (2020)

[25] Cheng, Q., Shen, J.: A new Lagrange multiplier approach for constructing structure preserving schemes, I. Positivity preserving. Computer Methods in Applied Mechanics and Engineering **391**, 114585 (2022)

[26] Cheng, Q., Shen, J.: A new Lagrange multiplier approach for constructing structure preserving schemes, II. Bound preserving. SIAM Journal on Numerical Analysis **60**, 970–998 (2022)

[27] Hong, Q., Li, J., Wang, Q.: Supplementary variable method for structure-preserving approximations to partial differential equations with deduced equations. Applied Mathematics Letters **110**, 106576 (2020)

[28] Gong, Y., Hong, Q., Wang, Q.: Supplementary variable method for thermodynamically consistent partial differential equations. Computer Methods in Applied Mechanics and Engineering **381**, 113746 (2021)

[29] Jing, X., Li, J., Zhao, X., Wang, Q.: Second order linear energy stable schemes for Allen-Cahn equations with nonlocal constraints. Journal of Scientific Computing **80**, 500–537 (2019)

[30] Okumura, M.: A stable and structure-preserving scheme for a non-local Allen-Cahn equation. Japan Journal of Industrial and Applied Mathematics **35**, 1245–1281 (2018)

[31] Hong, Q., Gong, Y., Zhao, J., Wang, Q.: Arbitrarily high order structure-preserving algorithms for the Allen-Cahn model with a nonlocal constraint. Applied Numerical Mathematics **170**, 321–339 (2021)

[32] Lee, H., Shin, J., Lee, J.: A high-order and unconditionally energy stable scheme for the conservative Allen-Cahn equation with a nonlocal Lagrange multiplier. Journal of Scientific Computing **90**, 1–12 (2022)

[33] Tang, T., Yang, J.: Implicit-explicit scheme for the Allen-Cahn equation preserves the maximum principle. Journal of Computational Mathematics **34**, 451–461 (2016)

[34] Wang, X., Kou, J., Gao, H.: Linear energy stable and maximum principle preserving semi-implicit scheme for Allen-Cahn equation with double well potential. Communications in Nonlinear Science and Numerical Simulation **98**, 105766 (2021)

[35] Li, D., Quan, C., Xu, J.: Stability and convergence of Strang splitting. Part I: scalar Allen-Cahn equation. Journal of Computational Physics **458**, 111087 (2022)

[36] Du, Q., Ju, L., Li, X., Qiao, Z.: Maximum principle preserving exponential time differencing schemes for the nonlocal Allen-Cahn equation. SIAM Journal on Numerical Analysis **57**, 875–898 (2019)

[37] Hou, T., Tang, T., Yang, J.: Numerical analysis of fully discretized Crank-Nicolson scheme for fractional-in-space Allen-Cahn equations. Journal of Scientific Computing **72**, 1214–1231 (2017)

[38] Liao, H., Tang, T., Zhou, T.: On energy stable, maximum-principle preserving, second-order BDF scheme with variable steps for the Allen-Cahn equation. SIAM Journal on Numerical Analysis **58**, 2294–2314 (2020)

[39] Gong, Y., Ji, B., Liao, H.: A maximum bound principle preserving iteration technique for a class of semilinear parabolic equations. Applied Numerical Mathematics **184**, 482–495 (2023)

[40] Quispel, G.R.W., McLaren, D.I.: A new class of energy-preserving numerical integration methods. Journal of Physics A: Mathematical and Theoretical **41**, 045206 (2008)

[41] Qiao, Z., Zhang, Z., Tang, T.: An adaptive time-stepping strategy for the molecular beam epitaxy models. SIAM Journal on Scientific Computing **33**, 1395–1414

(2011)

[42] Zhang, Z., Ma, Y., Qiao, Z.: An adaptive time-stepping strategy for solving the phase field crystal model. Journal of Computational Physics **249**, 204–215 (2013)